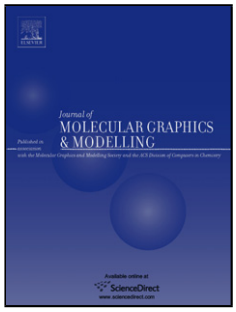

Title: Bioisosteric approach in designing new monastrol derivatives: An investigation on their ADMET prediction using in silico derived parameters

Author: Syed Fahad Hassan Umer Rashid Farzana Latif Ansari Zaheer -ul-Haq

PII: S1093-3263(13)00157-5
DOI: http://dx.doi.org/doi:10.1016/j.jmgm.2013.09.002
Reference: JMG 6333

To appear in: *Journal of Molecular Graphics and Modelling*

Received date: 28-5-2013
Revised date: 3-8-2013
Accepted date: 2-9-2013

Please cite this article as: Bioisosteric approach in designing new monastrol derivatives: An investigation on their ADMET prediction using in silico derived parameters, Journal of Molecular Graphics and Modelling (2013), http://dx.doi.org/10.1016/j.jmgm.2013.09.002

Bioisosteric approach in designing new monastrol derivatives: An investigation on their ADMET prediction using *in silico* derived parameters

Syed Fahad Hassan[1], Umer Rashid*[,2], Farzana Latif Ansari[3], Zaheer-ul-Haq[4]

[1]Department of Pharmacy, The University of Lahore, Defence Road Campus, Lahore 53700, Pakistan

[2]Department of Chemistry, Hazara University, Mansehra 21120, Pakistan

[3]Department of Chemistry, Quaid-i-Azam University, Islamabad 45320, Pakistan

[4]Dr. Panjwani Center for Molecular Medicine and Drug Research, International Center for Chemical Sciences, University of Karachi, Karachi 75270, Pakistan

*Corresponding author. Tel.: +92-997-414136

*E-mail: umer.rashid@hu.edu.pk; umer_rashid39@hotmail.com

Abstract

Medicinal chemists are facing an increasing challenge to deliver safer and more effective medicines. An appropriate balance between drug-like properties such as solubility, permeability, metabolic stability, efficacy and toxicity is one of the most challenging problems during lead optimization of a potential drug candidate. Insoluble and impermeable compounds can result in erroneous biological data and unreliable SAR in enzyme and cell-based assays. The weak inhibitory activity and non–drug-like properties of monastrol, the first small mitotic kinesin Eg5 inhibitor, has hampered its further development. In this investigation, a bioisosteric approach was applied that resulted in the replacement of C-5 carbonyl of monastrol with thio-carbonyl. Further lead optimization of drug-like properties was evaluated through *in silico* predictions by using ADMET predictor software. This minor structural modification resulted in upgraded Human effective jejunal permeability (Peff) and improved permeability in Madin-Darby Canine Kidney (MDCK) cells. Furthermore, C-5 thiocarbonyl analogue of monastrol (named as **Special-2**) was found safe to administer orally with no phospholipidosis toxicity, no raised levels of serum glutamate oxaloacetate transaminase (SGOT) and no potential towards cardiotoxicity. Molecular docking study was also carried out to understand the binding modes of these compounds. The docking study showed high binding affinity of the designed compounds against KSP. Hence a combination of in silico ADMET studies and molecular docking can help to improve prediction success and these compounds might be act as potential candidate for KSP inhibition.

Key words: Monastrol, Kinesin spindle protein, ADMET, Antimitotic, Bioisosterism

1. Introduction

The increasing number and diversity of methods has provided medicinal chemists with a powerful range of commercial and academic tools to aid in the optimization of lead compound activity and ADMET properties for drug design. Modulation and mediation of potency of a small drug-like molecule against its target is an important challenge in drug designing. Furthermore, its safety requirements and the surety that this drug-like molecule reaches its target effectively are also important. One of the most significant approaches to assist in efficiently navigating the available chemistry space is that of bioisosteric replacement. Bioisosteric transformations in a bioactive compound are generally used to replace group or groups of atoms that retain their specific activity or further improve its potency. Such chemical modifications are used in the process of compound exploration and lead optimization in order to enhance the desired biological and physical properties of potential drug candidates [1-4].

Antimitotic drugs such as taxanes and various vinca alkaloids are a major class of cytotoxic drugs in the treatment of cancer. Their targets are microtubules (MTs), which are composed of α- and β-tubulins [5,6]. Although these antimicrotubule drugs were successful in the treatment of cancer, however, their usage is limited due to their undesirable side effects such as neurotoxicity [6,7]. Kinesin spindle protein, (also called KSP or kinesin-5) has recently emerged as a promising target for a new generation of antimitotic chemotherapeutic agents [8]. Mayer *et al* reported the screening of a large library of compounds where racemic monastrol was identified as KSP inhibitor (IC_{50}=30 nM) and may be considered as a lead for the development of new anticancer drugs [9-11]. Following the discovery of monastrol, several other small molecules were reported as KSP inhibitors [8]. Although monastrol has been the prototype of KSP/Eg5 inhibitors, its relatively low cellular activity combined with other non-drug like properties has hampered its further development [12].

The computational approach, also known as *in silico* approach, is one of the most modern and fastest developing techniques, being used today in drug discovery, to assess the pharmacokinetics, ADME (absorption, distribution, metabolism, excretion) and toxicity predictions. The application of computational technology during drug discovery and development offers considerable potential for reducing the number of experimental studies required for compound selection and development and for improving the success rate. These

early predictions of ADMET properties help researchers to select the best candidates for drug development as well as to reject those with a low probability of success. The ultimate goal of the *in silico* ADMET properties is the prediction of the *in vivo* pharmacokinetics of a potential drug molecule in man, whilst it exists as only a virtual structure. This requires an integrated suite of models covering each of the processes involved and their incorporation into a full 'drug design' software package which combines ADME predictions with those for pharmacological properties, stability, chemical tractability, etc., to produce a molecule with the optimal combination of properties. This ideal, complete package does not yet exist, however, many of its component parts are already available and in some circumstances used for lead optimisation, screening an in drug design and development [13-17].

2. Results and discussions

Our interest in KSP inhibitors began when we identified monastrol as urease inhibitor in a structure based virtual screen (SBVS) experiment [18]. We also reported microwave assisted synthesis of ispinesib, the first KSP inhibitor in clinical trials [19]. Russowsky reported that monastrol displayed potent antitumor activity against many cell lines, with the thioxo-analogue (monastrol, **Special-1)** being more active than the oxo-analogue (**2**) and indicated the relative importance of sulphur atom for antiproliferative activity [20]. Keeping in view the importance of sulphur atom, we designed a C-5 thio-analogue of monastrol (**Special-2**) and illustrated how bioisosteric approach helps in an increase in drug-like properties. The compounds selected for current study include monastrol (Special-1), its oxo-analogue **2** and another dihydropyrimidine (DHPM) **3**. Moreover, bioisosters of monastrol designed by replacing C-5 carbonyl of DHPM scaffold by its thio-analogues Special-2 and 4 respectively were also studied. The structures of the compounds selected for ADMET properties are shown in **Fig. 1**.

Insert Fig. 1 here.

2.1. ADMET predictions

Setbacks have greatly outnumbered success in drug design and development process. In recent years we have seen a steady stream of drug candidates in development accompanied by a long series of unsuccessful outcomes. As research has intensified, a higher average of potential medicines pulled out of development each year has been observed. The importance of predicting

compound safety in humans has never been greater for the medicinal chemistry researcher considering these drug withdrawals mainly due to adverse effects and more rigorous regulatory requirements. In this context, computational approaches are used today to assess the ADMET properties of compounds at the early stages of drug discovery and development. In this study we evaluated drug-like properties of compounds through *in silico* predictions by using ADMET predictor software version 6.0 [21]. ADMET Predictor is an advanced computer program that enables researchers to rapidly predict a large number of ADMET properties from molecular structure. Its predictive models are grouped into metabolism, physicochemical and biopharmaceutical, toxicity and simulation modules. ADMET Predictor models have been consistently ranked as the most accurate, quick and useful tool to predict physico-chemical and biological properties of drug-like chemicals [22-30].

2.1.1. Absorption:

Drug absorption after oral administration, a convenient method for medication, is a very complicated process. Several types of descriptors have been proposed for this process. These include hydrophobicity (logP, and LogD, hydrogen bonding descriptors, polar surface area (PSA) and topological indices. Lipophilicity is an important property in an *in silico* model of absorption. For oral drug absorption, these *in silico* or theoretical models have been connected to simple molecular descriptors, for example lipophilicity, molecular weight, PSA and hydrogen bonding ability. Lipinski used these molecular properties in formulating his rule of five (Ro5) [31]. However, a major limitation of using these predictive rules is that many of the non-druggable compounds in commercially available screening libraries also obey these rules [32]. For these limitations, more sophisticated *in silico* models of absorption, frequently modelling activities in *in vitro* cell culture assays such as Caco-2, Madin-Darby Canine Kidney cells apparent permeability (MCDK) together with effective permeability (P_{eff}), have been developed [32-33].

Molecular descriptors of the designed **Special-1**, **Special-2** and DHPMs **2-4** were calculated using ADMET predictor. An inspection of the data given in **Table 1** reveals that all compounds obeyed Lipinski's Rule of five (RO5) and their molecular descriptors, such as Molecular weight (MW), LogP, hydrogen bond donor (HBD) and hydrogen bond acceptor (HBA) were found to comply with the cut off limits of Ro5. Predicted human jejunal permeability (P_{eff}) for both C-5

thio-analogues **Special-2** and **4** was greater than 0.1 cm/s × 10^4 and latter will show highest P_{eff} and MDCK permeability as shown in **Table 1**. However, effective permeability of oxo-monastrol (**2**) through intestinal membrane (0.01 cm/s ×10^4), reduced MDCK apparent permeability (86.53 cm/s×10^7) and logP (0.81) was found lower compared to monastrol. Difference in HBD/HBA count for **Special-1**, oxo-monastrol (**2**) and compound **3** was predicted to be greater emphasizing the importance of sulphur in these series of compounds [34]). Hence, the increased logP for C-5 thio-analogues, **Special-2** and **4**, showed improved P_{eff} and MDCK apparent permeability.

Insert Table 1 here.

Moreover, solubility of **Special-2** (0.39 mg/mL) was found to be slightly greater than **Special-1** (0.37 mg/mL) in simulated fasted state of intestinal fluid (**Table S-1** in Supporting Information). However, the solubility of **Special-2** in the simulated fasted state of gastric fluid and fed state intestinal fluid did not increase. Although, the solubility of **Special-1** in fed state of intestine was predicted to be 0.58 mg/mL, its decreased absorption and bioavailability may be ascribed to a decrease in permeability and logP. The solubility of other compounds is shown in the **Table S-1** of supporting information. Hence the **Special-2** can be given in the fasted state to absorb effectively in the duodenal/ jejunal portion of the small intestine. Moreover, due to increased log D for **Special-2** also promised its chance of absorption to be more than 50% if administered orally in accordance with molecular weight band distribution, as described in literature [35]. The absorption risk estimated by ADMET predictor™, showed as S+Deflt_Risk, also confers improved fraction absorbed for all compounds than monastrol and oxo-monastrol after oral administration, as reported in the literature (**Fig. 2**) [36].

Insert Fig. 2 here.

2.1.2. Distribution

Tissue distribution prediction of a drug is another important consideration in drug development. Molecular descriptors such as logP, molecular weight, pKa, logBBB have been proven to be useful in modelling distribution [37]. Volume of distribution (V_D) is another important parameter which relates the amount of a drug in the body to its measured concentration in a relevant

biological fluid or deep tissue compartment. It is defined as the volume in which a drug will appear to be distributed if it is presented throughout at the same concentration as that in plasma.

The distribution of all compounds under study with respect to volume of distribution (V_D) is approximately the same as shown in **Table 2**. This low volume of distribution (<5.5 L/kg) for all compounds ensured decreased deep tissue penetration, however, all compounds were predicted to distribute in a similar manner to total body water as the value of their V_D was greater than 0.7 L/kg [38]. Hence these compounds cannot be used for solid tumour. An inspection of the data given in **Table 2** revealed that **Special-1** and **Special-2** will remain in the blood for a longer period due to their high plasma protein binding (77.98 % and 84.99 % respectively) with their calculated log K value of -0.55 and -0.75 respectively, thereby reducing their chance of renal clearance [39]. Oxo-monastrol (**2**), on the other hand, was not expected to exhibit prolonged effect due to its low plasma protein binding (67.73 %) which abates its prolonged storage in blood and increased clearance from the body. The highest plasma protein binding was found for **4** in accordance with the highest logD and logP.

A decrease in unbound drug percentage of **Special-2** and **4** in the blood promised sustained or prolonged therapeutic outcome at receptor level along with the dependence on V_D. However, a direct relation to log D was seen with plasma protein binding of compounds. The higher the unbound drug concentration in plasma, the lesser the propensity to monitor it under controlled studies as therapeutic indices for **4** and **Special-2** is narrower than **Special-1**. Furthermore, a high protein binding of **Special-2** and **4** in plasma display long lasting effects and reduced dosing frequency. Sustainability was also supported by a high degree of renal absorption of **4** and **Special-2** over **Special-1** after renal clearance from distal parts of nephron due to increased log P of **4** and **Special-2**, co-supported by an increased logD and low renal excretion [40]. The relationship of LogD of **Special-1** and **Special-2** is shown in **Fig. 3**.

Insert Fig. 3 here.

It is predicted from above results that compounds with low V_D can be used to decrease the tumour growth in highly blood vessel perfused organs, like liver and spleen. The plasma protein binding of the compounds were predicted and correlated with the logD values of the compounds. Increasing logD has direct effect on the plasma protein binding of the compounds, i.e.

compounds having log D greater than 3 mostly exhibited greater than 90% plasma protein binding, as precedent in the literature [41]. The increase in logD is found promiscuous to directly relate with increased metabolic un-stability or clearance of the compound. The percentage of unbound drug present in the plasma was also predicted and then related with brain to plasma ($B/P_{unbound}$) ratio of **Special-2**. This ratio was predicted little higher than special-1 as depicted in the **Table 2.** However, logBBB and blood brain barrier penetration of both compounds was found to be low. Hence, both compounds cannot be used for the glioblastoma like deadly brain tumours, except in meningioma the penetration of compounds in the brain tissues can be considered.

Insert Table 2 here.

The propensity of all compounds towards P-glycoprotein (P-gp) was not very high, as supported by smaller logP, PSA and MW [42], while excess of oxo-monastrol (**2**), which was found to be more prone to P-gp due to its increased PSA and reduced basic pKa. Hence, it has reduced efficacy to evade the P-gp compared to other compounds. However, their increased HBD count will influence may increase efflux ratio *via* P-gp.

2.1.3. Metabolism

The process of biotransformation or metabolism is the enzymatic conversion of a drug to a metabolite. In the body, the metabolic enzyme concentration is constant at a given site, and the drug (substrate) concentration may vary. When the drug concentration is low relative to the enzyme concentration, there are abundant enzymes to catalyse the reaction, and the rate of metabolism is a first-order process. Cytochrome-P450s are the enzymes that catalyse the oxidation of organic substance. These are the major enzymes involved in drug metabolism. Most of the drugs undergo metabolism via cytochrome P450 (CYP) enzymes.

It may be seen from **Table 2** that **Special-2** and compound **4** have longer value of logD (2.71 and 2.36) respectively) which may be associated with an increased in metabolic instability. On the same grounds (**Table 2)** oxo-monastrol (**2)** may also be considered as metabolically instable compared to **Special-1** due to its higher logD. Metabolism of all compounds *via* Phase-I and Phase-II was predicted and all compounds were found to be metabolised *via* CYP3A4 and

CYP2D6. All the compounds were also metabolized *via* CYP2C19 isoform of the microsomal cytochrome P450 enzyme except oxo-monastrol (**2**). The enzyme CYP2C9 and CYP2C19 are genetic variant isoforms of cytochrome-P450 and expressed differently from population to population. The intrinsic clearance (Clint) of **Special-1** and **Special-2** were observed to be 4.037 and 2.201 μL/min/mg respectively that reflect slight genetic variance of therapeutic outcome from patient to patient (Caucasians, South Asians, Africans and Negroes etc), however, other compounds do not show significant genetic variance *via* CYP2C19 enzyme.

Further, **Special-1**, **Special-2** and oxo-monastrol (**2**) were predicted to be non-substrate for CYP1A2 and CYP2B6. This resulted in decreased metabolite conversion of parent compounds into high logP metabolites in the skin [43]. Therefore, these compounds were predicted to express good efficacy in metastatic or recurrent malignant melanoma where high expression of kinesin spindle proteins are found. In contrast, oxo-monastrol (**2**) has reduced effects in melanoma cell lines of UACC.62 due to decreased LogP as shown in **Table 2**. Compounds **3** and **4** showed a tendency to undergo metabolism in skin *via* CYP1A2 isoform and were converted into high logP metabolites which may have reduced effects in treating skin melanoma. However due to increase in logP they may penetrate into UACC.62 (melanoma) cell lines. Structures of all metabolites are given in Supporting Information.

Insert Table 3 here.

All compounds were predicted as substrates for CYP2D6 with compound **4** being a high substrate for CYP2D6 isoform as reflected from its highest Clint (31.39 μL/min/mg). Hence, it will interact with many commercially available marketed drugs known to be CYP2D6 inhibitors e.g. fluoxetine, paroxetine, quinidine, duloxetine, terbinafine, amiodarone, cimetidine, sertraline, celecoxib, chlorpheniramine, chlorpromazine, citalopram and other H_1-receptor antagonists. It may be seen from **Fig. 4** that **Special-2** is metabolized to Special-1 by the action of enzymes CYP2C19, CYP2C9, CYP2D6 and CYP3A4, therefore, concomitant use of these drugs should be avoided to facilitate this conversion of **Special-2**.

Insert Fig. 4 here.

All compounds may also undergo Phase-II metabolism to minor extent as their HBD are less than 4 [44]. The propensity of **Special-2** towards P-gp efflux transporter was very low, as it is a substrate for CYP3A4 with minor intrinsic clearance i.e. 1.895 µL/min/mg [45]. Hence these compounds will accumulate to some extent in bile canaliculi via this transporter. Similarly compound **4** is also less prone towards P-gp with reduced HBD count, PSA, MW and increased basic pKa. However, little proneness towards P-gp may occur due to slightly increased logP (**Table 1**) value which can be overcome by nephrotic reabsorption.

2.1.4. Clearance

The elimination of the compounds *via* renal clearance is mainly reflected by the distribution of compound in deep tissues. Moreover, passive clearance of drug also depends on % unbound drug in plasma and directly related to the elimination of drug via glomerular filtration. The estimation of the unbound percentage of drug is hence correlated to estimate the renal clearance of compounds in ml/min/kg. But this may vary depending upon the molecular weight of the compound, total polar surface area and active secretion of the compound being liable to P-gp efflux transporter.

Due to reduced molecular weights of all compounds (< 450 Da), their elimination is predicted to be driven mainly *via* renal corpuscle of kidney in urine [45]. However, because of an increase in LogD value of **Special-2**, **2** and **4**, the chance of metabolic clearance will increase [44]. However, active secretion *via* P-gp, present in the renal corpuscle, can enhance the renal clearance of all compounds. Hence, some amount of drug elimination products can also be found in faecal material, due to glucoronide conjugations, Phase-II metabolism and P-gp efflux transporters. The compound **3** also exhibited highest liability towards CYP3A4 metabolism, hence has increased propensity to eliminate actively *via* P-gp than compound **4** with reduced CYP3A4 clearance, as reported in literature [45].

2.1.5. Toxicity

ADMET risk for all compounds was predicted to be safe as shown in Table S-1 of Supplementary data. Among C-5 thio-analogues, Special-2 was found safest with ADMET risk=2 compared to compound **4** with ADMET risk=4. Oxo-monastrol (**2**) and **3**, however, possess low ADMET risk. Phospholipidosis estimations were predicted utilizing ADMET

Modeler of ADMET predictor™ software in which QSAR and computational toxicology models were built by FDA. All the compounds were found nontoxic and do not cause phospholipidosis. However, **Special-2** was found safe to administer orally with no phospholipidosis toxicity, no raised levels of serum glutamate oxaloacetate transaminase (SGOT) and no potential towards cardiotoxicity. Decreased cardiotoxicity is promised as is less prone towards Ether-à-go-go Related Gene (hERG) potassium channel [47]. ADMET space for all compounds is shown in **Fig. 5**.

Insert Fig. 5 here.

2.2. Molecular docking

Molecular docking has contributed a lot in the identification of novel small drug-like scaffolds exhibiting high binding affinity and selectivity for the target together with a reasonable ADMET profile. Such drug-like scaffolds are likely to be able to enter higher phases in the further drug development process. The binding modes of the compounds were predicted *via* molecular docking technique using Molecular Operating Environment (MOE) software [48]. As the first step, the crystal structure of protein complex of KSP was obtained from PDB (code 1Q0B). It contains Mg, one molecule of ADP bound in the nucleotide binding pocket and monastrol occupying an allosteric binding site as shown in **Fig. 6**. Jiang et al analysed binding mode of fifteen KSP inhibitors for the first time [49]. It was found that the binding site formed by two cooperative parts, the 'main pocket' is essential and the interaction of the inhibitor with the 'minor pocket' may greatly increase the bio-activity. Main pocket composed of Glu116, Gly117, Glu118, Arg119, Trp127, Asp130, Ala133, Ile136, Pro137, Tyr211, Glu215 and 'minor pocket' surrounded mainly by Ala218 and Arg221. They concluded that more potent inhibitors (with IC_{50} value <30 nM) shared a common character when binding to the KSP i.e. they all interact with a 'minor pocket in addition to the 'main binding pocket.

To investigate the binding mode of **Special-2**, we docked it into allosteric monastrol-bound Eg5 site. It was confirmed from the analysis of docking results that **Special-2** bound to the human Eg5 motor domain in an allosteric site previously described for other Eg5 inhibitors. It can be seen from **Fig. 6b** that 3-hydroxyl group of **Special-2** extended minor pocket surrounded mainly by Ala218 and Arg221 and showed interaction with Arg221. This additional interaction of

Special-2 with Arg221 may be considered as an important factor in making **Special-2** a strong and potential candidate for KSP inhibition. Moreover, **Special-1** exhibited the highest binding affinity (-10.0834 kcal/mol) compared to **Special-2** with binding energy in the range of -11.1876 kcal/mol that further confirmed its great potential as KSP inhibitor.

Insert Fig. 6 here

3. Conclusion

Drug designing is a many-faceted challenging problem that may be advanced by exploiting many tools. Bioisosterism is one of the most rapidly emerging tools that have led to the identification of many drug candidates. Exploiting the strength of this bioisosteric replacement, the designing of some derivatives of monastrol as KSP inhibitor has been carried out by a protocol followed involved the bioisosteric replacement of C-5 carbonyl of monastrol (designated as **Special-1**) leading to its derivative designated as **Special-2**. These compounds were further evaluated for their drug-like properties through *in silico* predictions by using ADMET predictor software. Our studies conclusively revealed that this minor structural modification resulted in upgraded ADMET properties. Furthermore, molecular docking studies were also performed in order to identify their binding affinity and binding energy towards KSP. Among all the studied compounds **Special-2** has shown highest binding affinity against KSP. Molecular docking studies also revealed that **Special-2** binds through Arg221 in the cooperative minor binding pocket which increases its binding affinity significantly. ADMET properties Special-1 (thioxo-analogue) and Compound 2 (oxo-analogue) were also compared with the experimental results in literature. Good correlations between the *in silico* ADMET predictions and experimental results was observed. We concluded that a combination of *in silico* ADMET studies and molecular docking can help to improve prediction success. Hence further analysis through *in vitro* and *in vivo* studies will prove that these compounds might be act as potential candidate for KSP inhibition.

4. Materials and Methods

4.1. ADMET predictions

In silico ADMET studies were performed by using ADMET predictor version 6.0 (Simulations Plus, Inc., Lancaster, CA, USA). Structures of the compounds were saved in the 'mol2' format

using MOE software. These 'mol2' files of molecular structures of compounds were uploaded into the ADMET predictor software for further evaluations. Various pharmacokinetic parameters like logP and LogD, hydrogen bonding descriptors, polar surface area (PSA), human intestinal absorption, plasma protein binding (PPB) etc. were estimated for all compounds at pH 7.4. The metabolites of the compound were generated by MedChem Designer^{TM} Software of Simulations-Plus using mol2 as input file.

4.2. Docking studies

MOE-Dock tool was employed to explore suitable binding conformations between small compounds and a macromolecular protein. It uses a Monte Carlo Simulated Annealing method for docking a ligand in the binding site of a receptor molecule. The program forms a 3D grid encompassing the canter of the docking site. The target compounds were built using the builder interface of the MOE program and subjected to energy minimization. The crystal structure of protein complex KSP with Mg^{2+}, NAD and monastrol was obtained from PDB (PDB ID 1Q0B). The edited crystal structure after removing water molecules was imported into MOE and all hydrogen atoms were added to the structure with their standard geometry followed by their energy minimization using MOPAC 7.0. The resulting model was subjected to systematic conformational search at default parameters with RMS gradient of 0.01kcal/mol using Site Finder. The enzyme was searched for its active site and dummy atoms were created from the resulting alpha spheres. The backbone and residues were kept fixed and the energy minimization was performed. Root mean square deviation (RMSD) values were used to compare the ligand between the predicted and its corresponding crystal structure. The resulting docked poses with RMSD less than 1.5Å were clustered together and the lowest energy minimized pose was used for further analysis. Ten different conformations were selected for each ligand. All other parameters were maintained at their default settings. The best conformation of each of the ligand-enzyme complex was selected based on energetic grounds. The resulting ligand-enzyme complex model was then used for calculating the energy parameters using MMFF94x force field energy calculation and predicting the ligand-enzyme interactions at the active site.

References

[1] H.J. Bohm, A. Flohr, M. Stahl, Scaffold hopping, Drug Discov. Today 1 (2004) 217–224.

[2] N. Brown, E. Jacoby, On scaffolds and hopping in medicinal chemistry, Mini Rev. Med. Chem. 6 (2006) 1217–1229.

[3] P. Ertl, In silico Identification of Bioisosteric Functional Groups, Curr. Opin. Drug Discov. Dev. 10 (2007) 281–288.

[4] C.G. Wermuth, In The Practice of Medicinal Chemistry (Ed: C. G. Wermuth), Academic Press, London, UK, (2003) 189–214.

[5] G.G. Gunderson, Evolutionary conservation of microtubule-capture mechanisms, Nat. Rev. Mol. Cell Biol. 3 (2002) 296-304.

[6] V. Sarli, A. Giannis, Targeting the Kinesin Spindle Protein: Basic Principles and Clinical Implications, Clin. Cancer Res. 14 (2008) 7583-7587

[7] E.K. Rowinski, V. Chaudhry, D.R. Cornblath, R.C. Donehower, Neurotoxicity of Taxol, J. Natl. Cancer Inst. 15 (1993) 107-115.

[8] H.B. El-Nassan, Advances in the discovery of kinesin spindle protein (Eg5) inhibitors as antitumor agents, Eur. J. Med. Chem. 62 (2013) 614–631.

[9] T.U. Mayer, T.M. Kapoor, S.J. Haggarty, R.W. King, S.L. Schreiber, T.J. Mitchison, Small molecule inhibitor of mitotic spindle bipolarity identified in a phenotype based screen, Science 286 (1999) 971-974.

[10] Z. Maliga, T.M. Kapoor, T.J Mitchison, Evidence that monastrol is an allosteric inhibitor of the mitotic kinesin Eg5. Chem. Biol. 9 (2002) 989-996.

[11] T.M. Kapoor, T.U. Mayer, M.L. Coughlin, T.J. Mitchison, Probing spindle assembly mechanisms with monastrol, a small molecule inhibitor of the mitotic kinesin, Eg5, J Cell Biol. 150 (2000) 975–988.

[12] M. Schmidt, H. Bastians, Mitotic drug targets and the development of novel anti-mitotic anticancer drugs, Drug Resist. Updates 10 (2007) 162–181.

[13] A. Boobis, U.G. Remy, P. Kremers, P. Macheras, O. Pelkonen, In silico prediction of ADME and pharmacokinetics Report of an expert meeting organised by COST B15, Euro. J. Pharm. Sci. 17 (2002) 183–193.

[14] T. Hou, J. Wang, W. Zhang, W. Wang, X. Xu, Recent Advances in Computational Prediction of Drug Absorption and Permeability in Drug Discovery, Curr. Med. Chem. 13 (2006) 2653-2667.

[15] D. Hecht, G.B. Fogel, Computational Intelligence Methods for ADMET Prediction. Front. Drug Des. Discovery, 4 (2009) 351-377.

[16] G. Moroy, V.Y. Martiny, P. Vayer, B.O. Villoutreix, M.A. Miteva, Toward in silico structure-based ADMET prediction in drug discovery, Drug Disc. Today 17 (2012) 44-55.

[17] N.A. Hosea, H.M. Jones, Predicting Pharmacokinetic Profiles Using in Silico Derived Parameters, Mol. Pharmaceutics 10 (2013) 1207−1215.

[18] U. Rashid, I. Batool, A. Wadood, A. Khan, Zaheer-ul-Haq, M.I. Chaudhary, F.L. Ansari, Structure based virtual screening-driven identification of monastrol as a potent urease inhibitor. J. Mol. Graphics Modell. 43 (2013) 47-57.

[19] U. Rashid, Ahsanullah, M. Waseem, F.L. Ansari, Microwave assisted partial synthesis of enantiomerically pure S-ispinesib-A case study, J. Chem. Soc. Pak. 35 (2013) 846-858.

[20] D. Russowsky, R.F.S. Canto, S.A.A. Sanches, M.G.M. D'Oca, A. Fatima, R.A. Pilli, L.K. Kohn, M.A. Antonio, J.E. Carvalho, Synthesis and differential antiproliferative activity of Biginelli compounds against cancer cell lines: monastrol, oxo-monastrol and oxygenated analogues, Bioorg. Chem. 34 (2006) 173-182.

[21] ADMET Predictor™ version 6, Simulations Plus, Inc. Lancaster, CA, USA. www.simulations-plus.com.

[22] J.C. Dearden, In silico prediction of aqueous solubility, Expert Opin. Drug Discovery, 1 (2006) 31-52.

[23] I.V. Tetko, G.I. Poda, Molecular drug properties: Measurement and prediction." ed. Mannhold R., Weinheim, Germany, Wiley-VCH (2007) 381-406.

[24] R. Mannhold, G.I. Poda, C. Ostermann, I.V. Tetko, Calculation of molecular lipophilicity: State of the Art and comparison methods, J. Pharm. Sci. 98 (2008) 84.

[25] J. Oyarzabal, J. Pastor, T.J. Howe, Optimizing the performance of in silico ADMET general models according to local requirements, J. Chem. Model 49 (2009) 2572.

[26] S.C. Sydney, S.K. Jae, G.V. Luis, S.Na kissa , In silico modeling to predict drug-induced phospholipidosis. Toxicol. Appl. Pharmacol. (2013) http://dx.doi.org/10.1016/j.taap.2013.03.010

[27] K. Makiko, T. Kouta, M. Kazuya, H. Yuka, I. Satoki, C. Koji, A. Yutaka, S. Yuichi, In Silico classification of major clearance pathways of drugs with their physiochemical parameters Drug Metab. Dispos. 38 (2010) 1362–1370.

[28] W. Sarah, A. May, N. A. Bou-Chacra, G. L. Amidon, B.-J. Lee, J. Feng, I. Kanfer, J.Z. Zuo, H. Wei, M.B. Bolger, R. Lobenberg, Provisional biopharmaceutical classification of Some common herbs used in Western Medicine, Mol. Pharmaceutics 9 (2012) 815−822.

[29] J. Kirchmair, A. Bender, M.J. Williamson, R.C. Glen, J.D. Tyzack, L. Tan, P.J. Bond, Computational prediction of metabolism: Sites, Products, SAR, P450 enzyme dynamics and mechanisms, J. Chem. Inf. Model. 52 (2012) 617−648.

[30] R. Mannhold, G.I. Poda, C. ostermann, I.V. Tetko, Calculation of molecular lipophilicity: State-of-the-Art and comparison of Log P methods on more than 96,000 compounds, J. Pharm. Sci. 98 (2009) 861-893.

[31] C.A. Lipinski, Drug-like properties and the causes of poor solubility and poor permeability, J. Pharmacol. Toxicol. Methods 44 (2000) 235-49.

[32] T. Hou, J. Wang, W. Zhang, W. Wang, X. Xu, Recent advances in computational prediction of drug absorption and permeability in drug discovery, Curr. Med. Chem. 13, (2006) 2653-2667.

[33] H. Lennernas, Human intestinal permeability, J. Pharm. Sci. 87 (1998) 403–410.

[34] D.A. Smith, D.S. Millan, Future Targets and Chemistry and ADME Needs, Metabolism, Pharmacokinetics and Toxicity of Functional Groups: Impact of Chemical Building Blocks on ADMET, Royal Soc. Chem. (2010) 507.

[35] M.J. Waring, Defining optimum lipophilicity and molecular weight ranges for drug candidates-Molecular weight dependent lower log D limits based on permeability, Bioorg. Med. Chem. Lett., 19 (2009) 2844-2851.

[36] Y.H. Zhao, J. Le, M.H. Abraham, A. Hersey, P.J. Eddershaw, C.N. Luscombe, D. Boutina, G. Beck, B. Sherborne, I. Cooper, J.A. Platts, Evaluation of Human Intestinal Absorption Data and Subsequent Derivation of a Quantitative Structure-activity Relationship (QSAR) with the Abraham Descriptors. J. Pharm. Sci. 90 (2001) 749–784.

[37] P. Poulin, K. Schoenlein, F.P. Theil, Prediction of adipose tissue: plasma partition coefficients for structurally unrelated drugs, J. Pharm. Sci., 90 (2001) 436-447.

[38] D.A. Smith, D.S. Millan, Metabolism, Pharmacokinetics and Toxicity of Functional Groups: Impact of Chemical Building Blocks on ADMET, Royal Society of Chemistry. (2010) 78.

[39] Y. Yang, O. Engkvist, A. Llinàs, H. Chen, Beyond Size, Ionization State, and Lipophilicity: Influence of Molecular Topology on Absorption, Distribution, Metabolism, Excretion, and Toxicity for Drug-like Compounds, J. Med. Chem. 55 (2012) 3667-3677.

[40] D.A. Smith, H. Waterbeemd, D.K. Walker, Pharmacokinetics and Metabolism in Drug Design. Wiley-VCH: Weinheim, Germany, (2001)

[41] H. Waterbeemd, D.A. Smith, B.C. Jones, Lipophilicity in PK design: methyl, ethyl, futile, J. Comput. Aided Mol. Design 15 (2001) 273-286.

[42] S.A. Hitchcock, Structral modification that alter the P-glycoprotein eflux properties of compounds, J. Med. Chem. 55 (2012) 4877-4895.

[43] J. Kirchmair, A. Howlett, J.E. Peironcely, D.S. Murrell, M.J. Williamson, S.E. Adams, T. Hankemeier, L. Buren, G. Duchateau, W. Klaffke, R.C. Glen, How Do Metabolites Differ from Their Parent Molecules and How Are They Excreted?, J. Chem. Inf. Model. 53 (2013) 354-367.

[44] J.R. Proudfoot, The evolution of synthetic oral drug properties, Bioorg. Med. Chem. Lett. 15 (2005) 1087-1090.

[45] T.J. Raub, P-glycoprotein recognition of substrates and circumvention through rational drug design, Mol. Pharm. 3 (2006) 3-25.

[46] W.J. Egan, Predicting ADME properties in drug discovery, in Drug design: structure- and ligand-based appraoches, K.M. Merz, D. Ringe, and C.H. Reynolds, Editors. Cambridge University Press: New York, USA. (2010) 165-173.

[47] R. Pearlstein, R. Vaz, D. Rampe, Understanding the structure- activity relationship of the human ether-a-go-go-related gene cardiac K^+ channel: a model for bad behaviour, J. Med. Chem. 46 (2003) 2017-2022.

[48] Molecular Operating Environment (MOE), 2012.10; Chemical Computing Group Inc., 1010 Sherbooke St. West, Suite #910, Montreal, QC, Canada, H3A 2R7, 2012.

[49] C. Jiang, Y. Chen, X. Wang, Q. You, Docking studies on kinesin spindle protein inhibitors: An important cooperative 'minor binding pocket' which increases the binding affinity significantly, J. Mol. Model. 13 (2007) 987–992.

[50] E. F. Pettersen, T.D. Goddard, C.C. Huang, G.S. Couch, D.M. Greenblatt, E.C. Meng, T. E.Ferrin, UCSF Chimera - A visualization system for exploratory research and aAnalysis. J. Comput. Chem. 25 (2004) 1605-1612 .

Figure captions

Fig. 1. 2D chemical structures of the molecules used to predict ADMET properties

Fig. 2. Predicted effective human jejunal permeability

Fig. 3. Special-2 depicting increased plasma protein binding and potency over Special-1 with narrow therapeutic index and sustain effect

Fig. 4. Metabolites of a) **Special-1** and b) **Special-2**

Fig. 5. ADMET space for all compounds under study by using 4D data mining tool of ADMET predictor software

Fig. 6. Modelled mode of binding of compounds in KSP active site. a) 3D hydrophobicity surface view of Special-1 (right), 2D binding interactions (left), b) 3D hydrophobicity surface view of Special-2 (right), 2D binding interactions (left). The hydrophobicity surface view is rendered from the program UCSF Chimera [50]

Tables

Table 1. Permeability of monastrol and its C-5 thio-analogue.

No.	HBD at $pH_{7.4}$	HBA at $pH_{7.4}$	Difference in HBD/HBA*	Peff cm/s $\times 10^{4}$	MDCK cm/s $\times 10^{7}$	logP	Ro5
Special-1	3	5	2	0.1	166.5	1.83	0
Special-2	3	4	1	0.47	231.93	2.00	0
2	3	6	3	0.01	86.53	0.81	0
3	2	4	2	0.16	148.23	2.59	0
4	2	3	1	0.81	271.49	2.36	0

*HBD/HBA= hydrogen bond donor/acceptor sites at physiological pH of 7.4.

Table 2. P-glycoportein propensity of special-1 and special-2 of the compounds sttudied.

No.	logD	V_D L/kg	% Unbound	Log K	pKa	logP	PSA	MW	HBD	Peff cm/s×10^4	$B/P_{unbound}$ ratio	logBBB	BBB Filtering
Special-1	1.82	0.89	22.02	-0.55	9.45	1.83	70.60	292.36	3	0.1	6.9	-0.26	Low
Special-2	2.71	0.9	15.01	-0.75	9.87	2.00	53.50	308.42	3	0.47	10.7	-0.3	Low
2	1.87	0.87	32.27	-0.32	9.00	0.81	87.70	276.29	3	0.01	27.89	-0.11	High

3	2.21	0.98	21.15	-0.57	9.54	2.22	50.40	276.36	2	0.22	9.50	-0.23	Low
4	2.36	0.97	14.19	-0.78	9.98	2.36	33.30	292.42	2	0.81	9.44	-0.41	Low

Table-3 Metabolism of all compounds *via* hepatic microsomal isoforms

No.	CYP1A2	CYP2B6	CYP2C19	CYP2C19 CLint µL/min/mg	CYP2D6	CYP2D6 CLint µL/min/mg	CYP3A4	CYP3A4 Clint µL/min/mg
Special-1	NS	NS	-/+	4.037	+	9.71	-	3.159
Special-2	NS	NS	-/+	2.201	+	14.57	-/+	1.895
2	NS	NS	NS	Nil	NS	Nil	+	3.264
3	+	NS	-/+	0.404	+	23.55	-/+	25.431
4	+	NS	-/+	0.225	+	31.39	-/+	8.06

Inhibition of CYP isoform = (-) Substrate for CYP isoform = (+) Partial agonist = (-/+) Nil = less or no propensity towards isoform NS = non-substrate for isoform, This data was generated by ADMET predictor™ software.

Graphical Abstract

Bioisosteric approach in designing new monastrol derivatives: An investigation on their ADMET prediction using in silico derived parameters

Syed Fahad Hassan[1], Umer Rashid*[,2], Farzana Latif Ansari[3], Zaheer-ul-Haq[4]

[1]Department of Pharmacy, The University of Lahore, Defence Road Campus, Lahore 53700, Pakistan

[2]Department of Chemistry, Hazara University, Mansehra 21120, Pakistan

[3]Department of Chemistry, Quaid-i-Azam University, Islamabad 45320, Pakistan

[4]Dr. Panjwani Center for Molecular Medicine and Drug Research, International Center for Chemical Sciences, University of Karachi, Karachi 75270, Pakistan

*Corresponding author. Tel.: +92-997-414136

*E-mail: umer.rashid@hu.edu.pk; umer_rashid39@hotmail.com

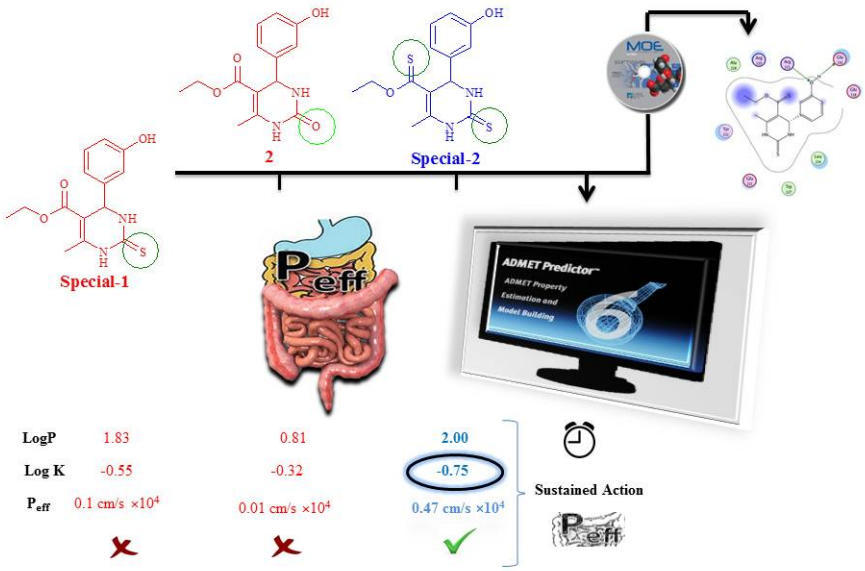

Highlights

Monastrol, a thioxo analogue, being more active than the oxo-analogue

This indicated the importance of the sulphur for the antiproliferative activity

Therefore bioisosteric replacement of C-5 carbonyl of monastrol with thio-carbonyl

This minor structural modification resulted in upgraded ADMET properties

Docking study was also performed to improve prediction success.

Figure(s)

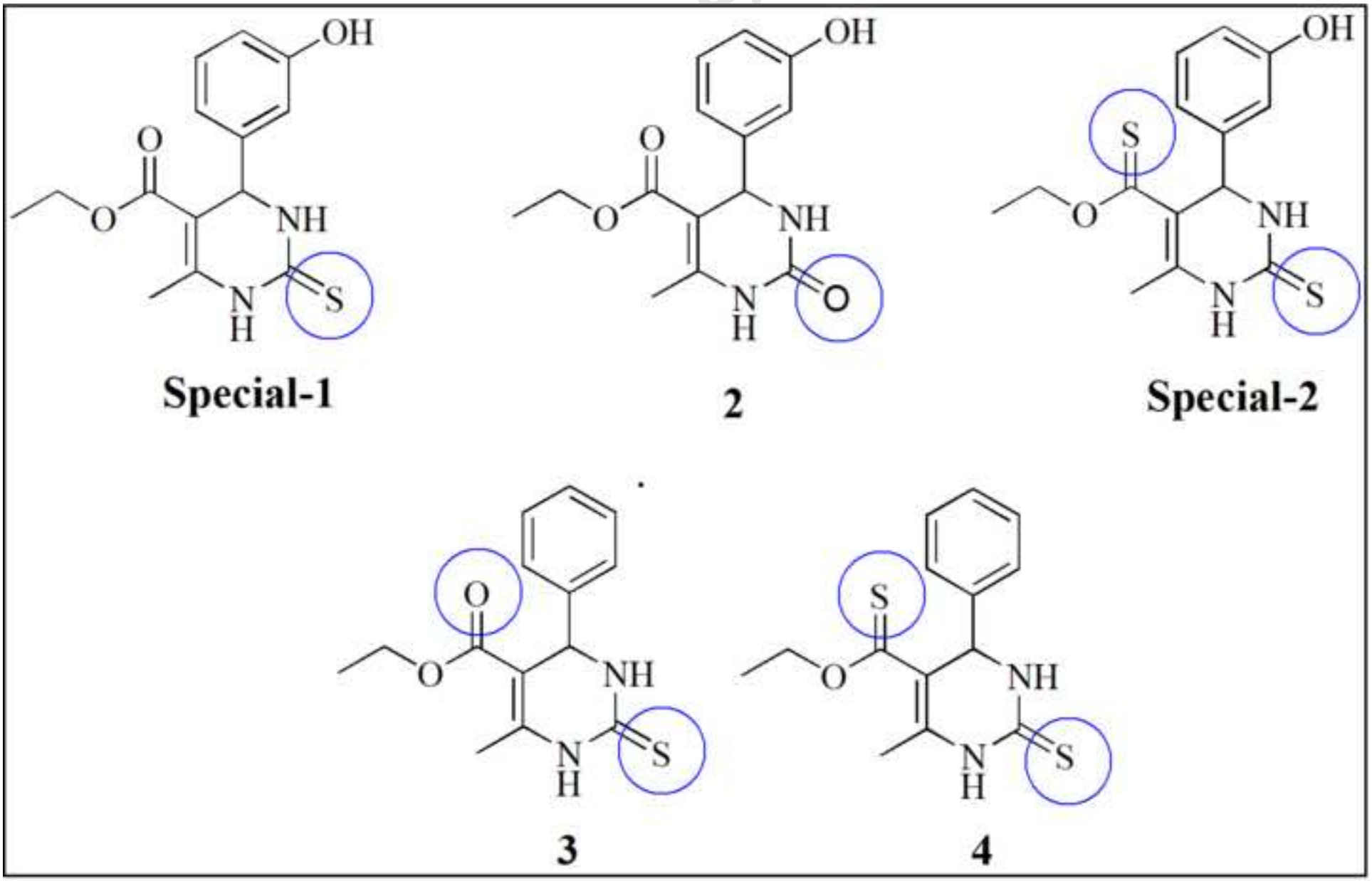
OH
O
O
NH
N
H
S
Special-1
OH
O
O
NH
N
H
O
2
OH
S
O
NH
N
H
S
Special-2
O
O
NH
N
H
S
3
S
O
NH
N
H
S
4

Figure(s)

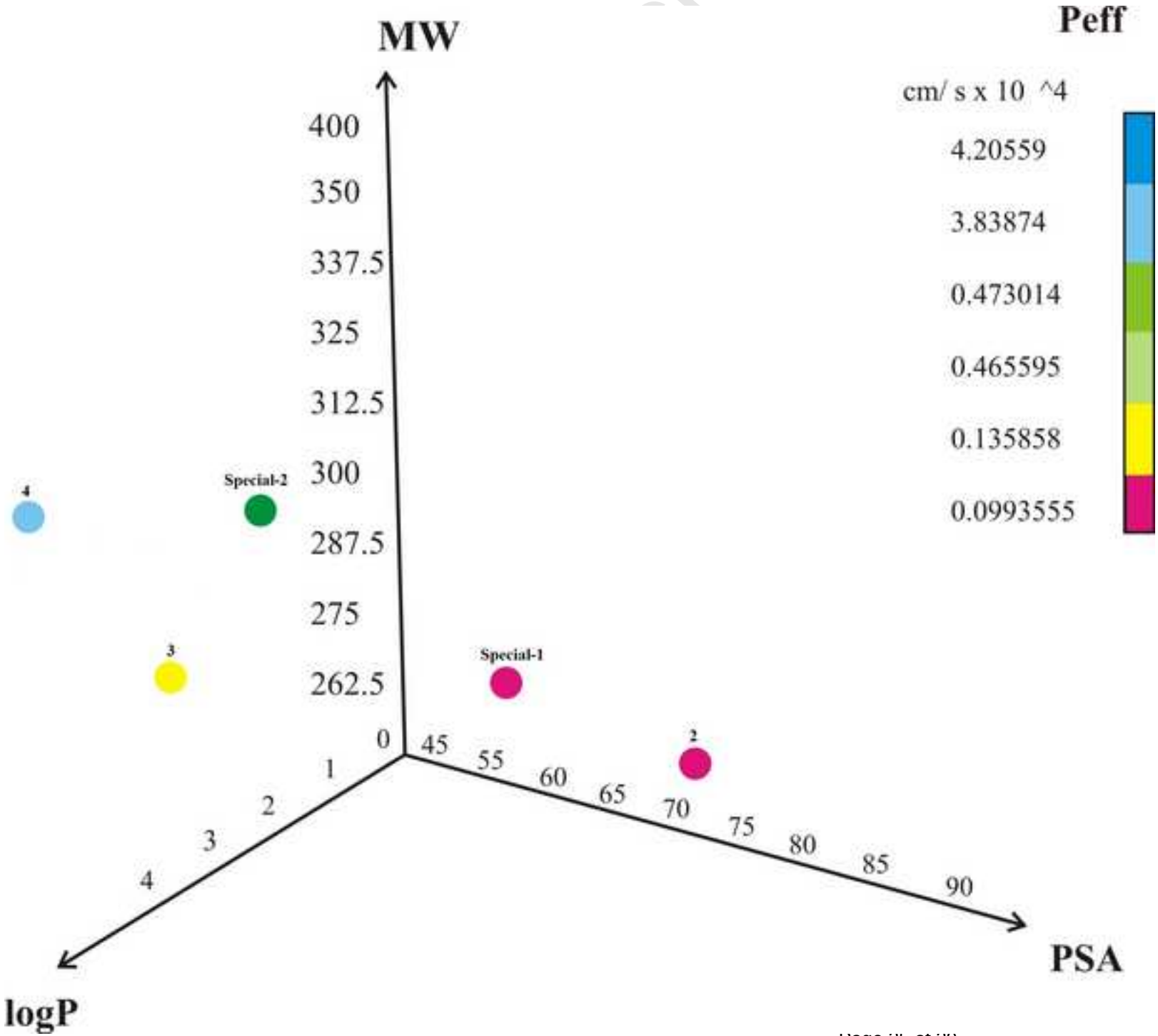
MW
Peff
cm/ s x 10 ^4
4.20559
3.83874
0.473014
0.465595
0.135858
0.0993555
400
350
337.5
325
312.5
300
287.5
275
262.5
Special-2
4
3
Special-1
2
0
1
2
3
4
45
55
60
65
70
75
80
85
90
logP
PSA

Figure(s)

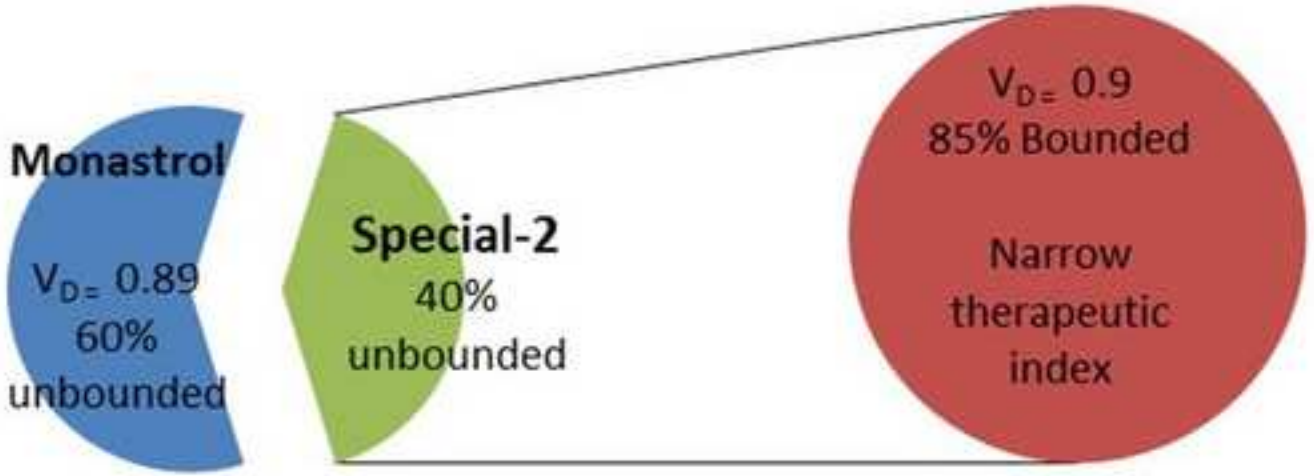
Monastrol
$V_{D=}$ 0.89
60%
unbounded
Special-2
40%
unbounded
$V_{D=}$ 0.9
85% Bounded
Narrow
therapeutic
index

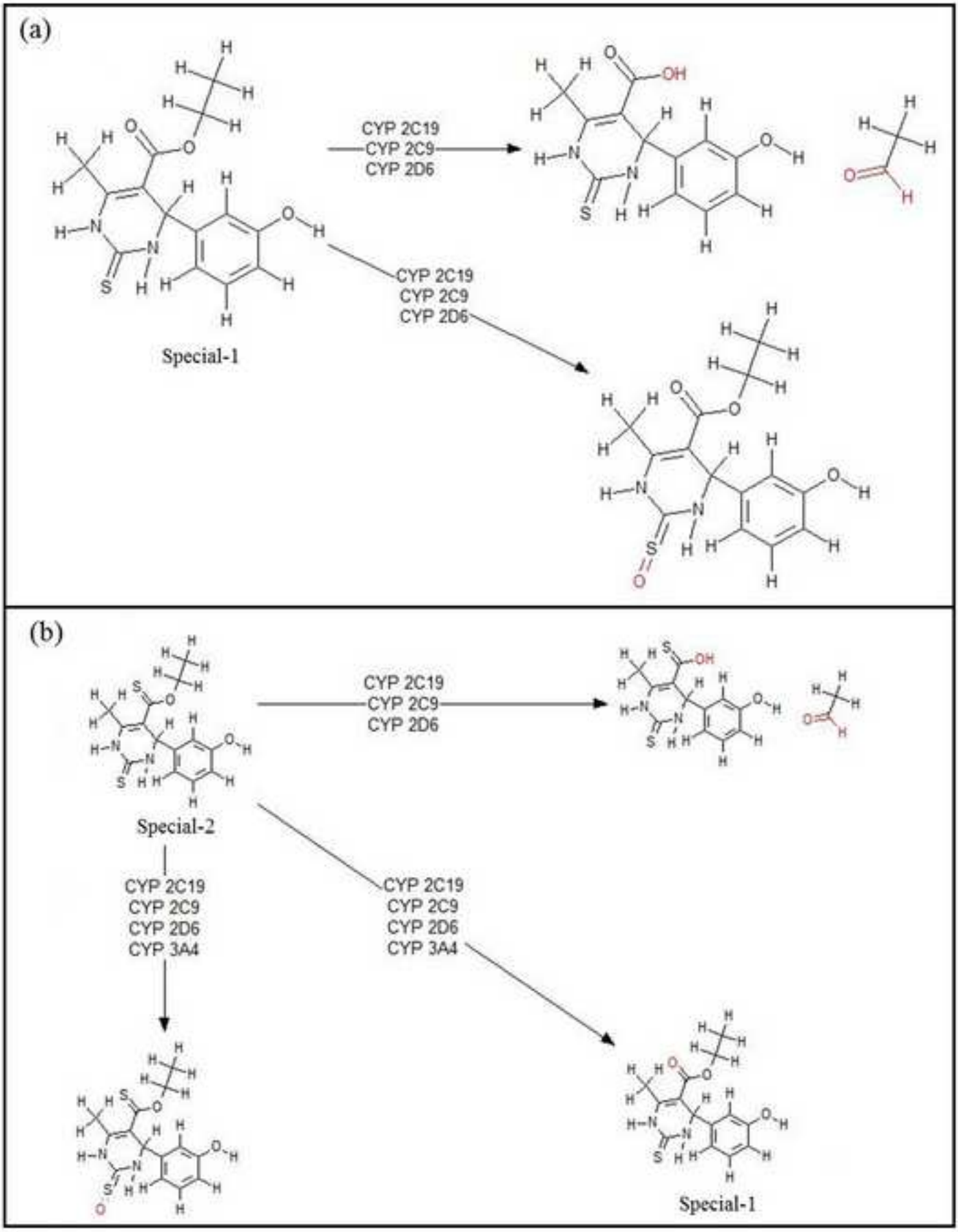

Figure(s)

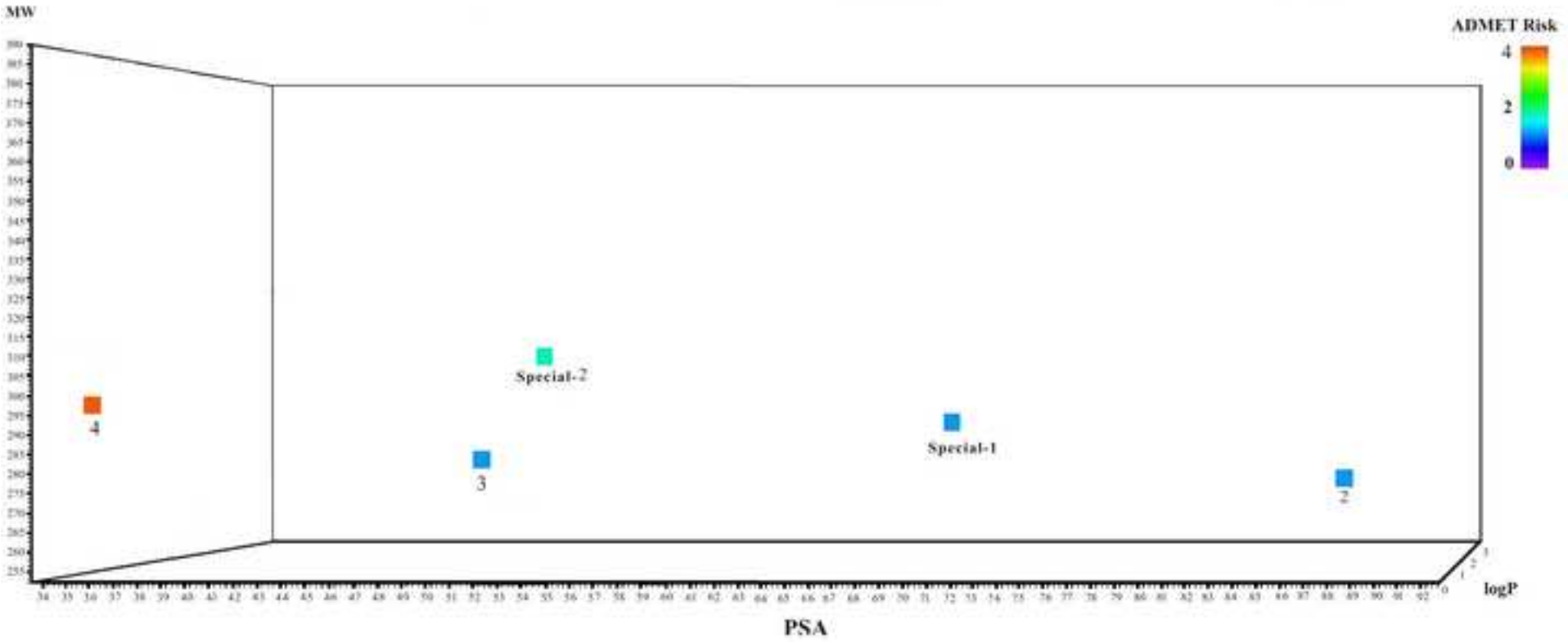

Figure(s)

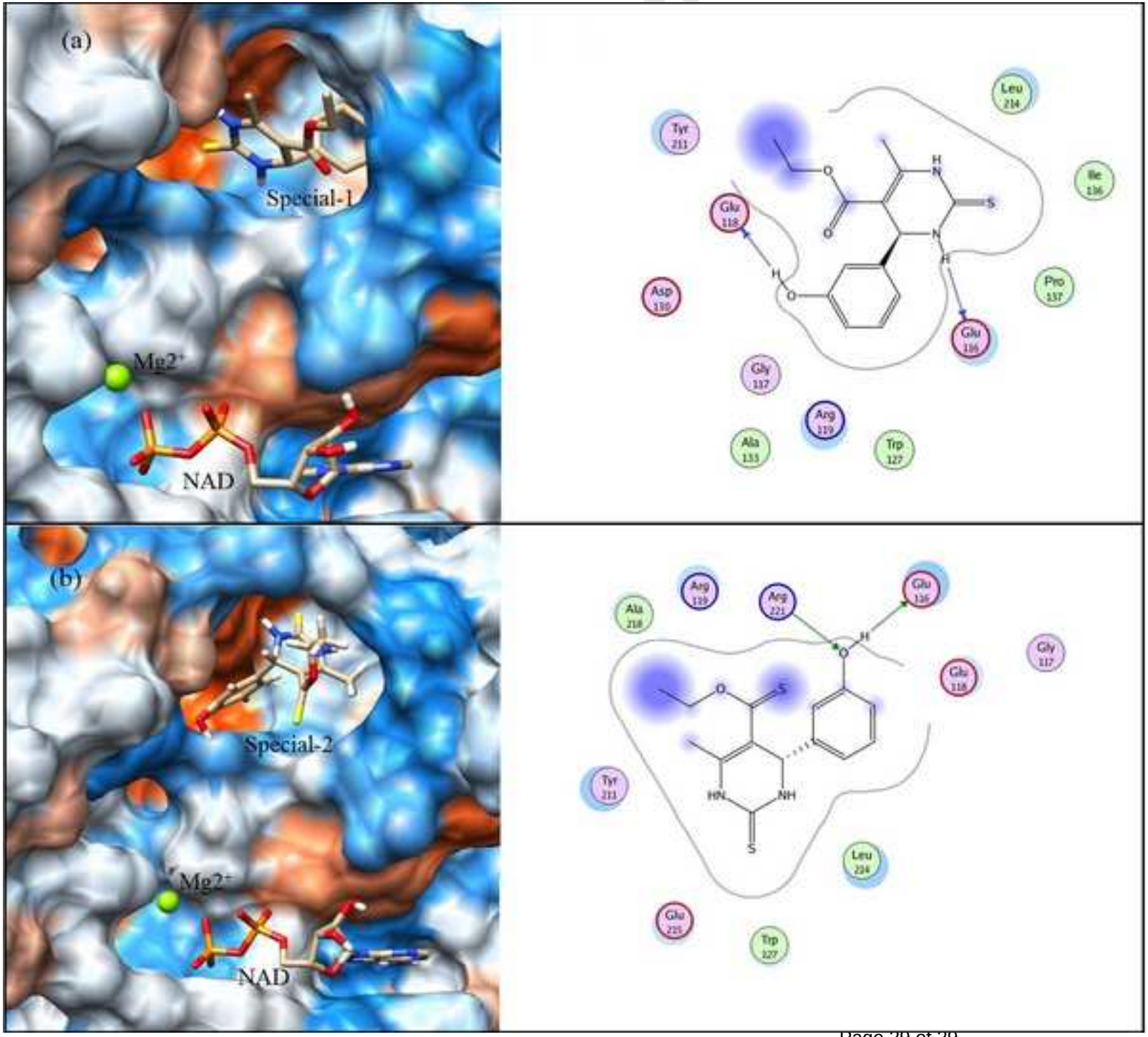
(a)
Special-1
Mg2+
NAD
Leu 214
Tyr 211
Ile 136
Glu 116
Asp 110
Pro 137
Glu 156
Gly 117
Arg 119
Ala 155
Trp 127
(b)
Special-2
Mg2+
NAD
Arg 119
Arg 221
Glu 156
Ala 218
Gly 117
Glu 118
Tyr 211
Leu 214
Glu 225
Trp 127